Adsorptive endocytosis and membrane recycling by cultured primary bovine brain microvessel endothelial cell monolayers

THOMAS J. RAUB*

Drug Delivery Systems Research, 7271-209-623, The Upjohn Company, 301 Henrietta St, Kalamazoo, MI 49001, USA

and KENNETH L. AUDUS

Department of Pharmaceutical Chemistry, University of Kansas, Lawrence, KS 66045, USA

* Author for correspondence

Summary

The dynamics of membrane recycling were examined in primary cultures of brain microvessel endothelial cells (BMECs). Because the BMEC surface was dominated by galactosylated glycoconjugates, ricin agglutinin (RCAI) was used as a tracer to follow the endocytosis and recycling of RCAI binding sites. These binding sites accounted for 75% of the iodinatable or most externally disposed plasma membrane proteins. Because greater than 90% of the RCAI that had bound to BMECs was removed by a brief, nontoxic treatment with galactose, the amounts and kinetics for internalization and efflux of [^{125}I]RCAI were measured. Both endocytosis and efflux were energy dependent. By using pseudo-first-order kinetics, the $t_{\frac{1}{2}}$ values for RCAI binding, internalization and efflux were 5, 18 and 13–14 min, respectively. By comparing efflux with and without galactose present, we found that 60% of the RCAI binding sites that had been internalized were returned to the cell surface and reinternalized. Quantifying the distribution of gold–RCAI following internalization showed kinetics consistent with that obtained using radiolabeled RCAI. Both horseradish peroxidase (HRP) and gold-conjugated RCAI that had bound BMEC at 4°C became localized within more caveolae within 2.5 min of warming to 37°C to permit endocytosis. With time, RCAI appeared within endosomes and tubules and vesicles of which some were located in the *trans*-Golgi network (TGN). The distribution of HRP–RCAI contrasted with that of free HRP, which was not routed to the TGN. The absence of RCAI conjugates in association with the basolateral membrane domain suggested the presence of functional tight junctions and maintenance of polarity throughout the duration of these experiments. These results showed that membrane recycling was more extensive and much slower than fluid-phase endocytosis in cultured BMECs. Moreover, we found that endocytosis of membrane by BMECs in culture was similar to that reported for brain endothelium *in vivo* in that a fraction of the cell surface membrane was routed to the TGN.

Key words: blood–brain barrier, brain, endocytosis, endothelial cell, microvessel, recycling, ricin agglutinin, *trans*-Golgi network.

Introduction

The capillary endothelium that contributes to the blood–brain barrier (BBB) is emerging as a uniquely dynamic and metabolically active cell barrier that protects and at the same time communicates with the central nervous system. The ability of the microvessel endothelium to regulate the movement of blood-borne proteins by exclusion or by selective transport pathways is generating a vast interest in characterizing the brain microvessel endothelial cell (BMEC) with regard to plasma membrane composition and the cell's capacity to accumulate and/or transport macromolecules by endocytosis (Pardridge, 1988; Brightman, 1989). With the development of *in vitro* models that include isolated microvessel capillaries (Goldstein *et al.* 1984; Pardridge *et al.* 1985) and cultured BMECs (Bowman *et al.* 1983; Audus and Borchardt, 1986; Audus and Borchardt, 1987), transport pathways are being studied at the cellular level.

Reese and Karnovsky (1967) first demonstrated by using horseradish peroxidase (HRP) that BMECs *in situ* had less fluid-phase pinocytic activity relative to endothelia from other capillaries and this attribute became an identifying hallmark. While characterizing the *in vitro* model for use in transport studies, we became interested in the kinetics of fluid-phase endocytosis and showed that cultured BMECs also exhibited a low capacity for solute accumulation (Guillot *et al.* 1990). During that study, it was apparent that these cells were quite active with regard to membrane traffic or retrieval and recycling of the apical or blood-side plasma membrane. Little is known about endocytosis and membrane traffic within BMECs. Broadwell *et al.* (1988) recently showed for the first time by using a lectin conjugate that BMECs *in vivo* possess an intricate

Journal of Cell Science 97, 127–138 (1990)

endocytic membrane system that involves prelysosomal compartments including those associated with the *trans*-most Golgi cisternae.

As an adjunct to our previous work on fluid-phase endocytosis and to examine further membrane rather than solute traffic following endocytosis, we employed the lectin, Ricin communis agglutinin I (RCAI), as a tracer of adsorptive endocytosis. Isolated from the castor bean, RCAI is a glycoprotein with a molecular weight of 120×10^3 that binds carbohydrates that contain β-D-galactosyl or β-D-*N*-acetylgalactosaminyl residues (Olsnes *et al.* 1974). Because RCAI binds reversibly to cell surface proteins and glycolipids, internalization and recycling of these lectin binding sites could be followed quantitatively and qualitatively by using radiolabeled and electron-dense conjugates of RCAI.

Materials and methods

Cell isolation and culture

Bovine BMECs were isolated from gray matter of the cerebral cortex as described previously (Audus and Borchardt, 1986) and stored frozen at −135°C in 10% (v/v) dimethylsulfoxide prior to use. For culture, cells were plated onto plastic that had been coated with 1.5 mg ml^{-1} (0.17 mg cm^{-2}) rat tail collagen (Biomedical Technologies, Inc., Stoughton, MA), subsequently crosslinked in a saturated NH_4OH atmosphere for 5 min and air dried, and 25 μg ml^{-1} (4–5 μg cm^{-2}) human fibronectin (Boehringer-Mannheim Biochemicals, Indianapolis. IN) at a density of 50 000 cells cm^{-2} in culture medium (Guillot *et al.* 1990) containing 120 μg ml^{-1} heparin (162 USP units mg^{-1}; Sigma Chemical Co., St Louis, MO). Cultures were maintained in a humidified mixture of 95% air and 5% CO_2 at 37°C and the medium was replaced every other day. After the formation of confluent cell monolayers within 10–12 days, experiments were carried out as described below. The purity of these cultures has been demonstrated elsewhere (Audus and Borchardt, 1986; Baranczyk-Kuzma *et al.* 1986; Baranczyk-Kuzma *et al.* 1989; Guillot *et al.* 1990).

Established cultures of bovine brain and adrenal microvessel endothelial cells (a gift to The Upjohn Company from Dr Gospodarowicz, University of California Medical Center, San Francisco) were maintained as described (Gospodarowicz *et al.* 1986). Madin-Darby bovine kidney epithelial cells (ATCC CCL 22) were grown in modified McCoy's 5A medium containing 10% (v/v) heat-inactivated newborn calf serum.

Iodination of RCAI

Ricinus communis agglutinin (RCAI or RCA_{120} from Vector Laboratories, Inc., Burlingame, CA) at 0.5 mg ml^{-1} in 200 μl phosphate-buffered saline, pH 7.4 (PBS), containing 0.1 M galactose was iodinated by addition of two Iodo-Beads™ (Pharmacia, Piscatawy, NJ) and 1.0 mCi of $Na^{125}I$ (carrier-free; Amersham Corp., Arlington Heights, IL). After 10 min at 4°C, free ^{125}I was removed by gel filtration. Samples of the void volume were dialyzed against PBS prior to use. Under these conditions, specific activity of the lectin was 2–4 μCi μg^{-1} protein.

Binding of [^{125}I]RCAI to BMEC monolayers

Confluent cell monolayers in 24-well plates (approximately 6×10^5 to 7×10^5 cells/well) were preincubated for 30 min at 37°C in serum-free medium (SFM) prior to each experiment to remove adsorbed serum proteins. After rinsing with ice-cold SFM, the cells were incubated for 20 min at 4°C in 0.5 ml SFM containing 0.1 mg ml^{-1} bovine serum albumin (SFM/BSA) and [^{125}I]RCAI (0.6 μg ml^{-1} or 5 nM) alone, or with increased concentrations of unlabeled RCAI to determine the saturation curve of binding. The labeling medium was decanted and counted by gamma spectrometry. After washing the cells twice with 1 ml ice-cold PBS, the labeled cells were solubilized with 1 ml of 2% (w/v) sodium carbonate, 0.4% (w/v) sodium hydroxide, 0.16% (w/v) sodium tartrate and 1% (w/v) sodium dodecyl sulfate (SDS) and total cell-associated radioactivity and total protein (Markwell *et al.* 1981) were measured.

Each experiment comprised three or four wells per data point and used two different iodinated preparations. All values were expressed as the amount of total radioactivity that was cell-associated after correction for nonspecifically cell-associated radioactivity or that which had bound in the presence of 0.1 M galactose. Greater than 95% of the radioactivity was bound specifically.

Internalization of [^{125}I]RCAI

Confluent monolayers were allowed to bind and internalize [^{125}I]RCAI (2.5 nM) for up to 4 h by continuous incubation in SFM/BSA at 37°C. To distinguish binding from uptake, the labeling medium was decanted, the cells rinsed once with ice-cold PBS, and surface-associated radioactivity was removed quantitatively with two 2.5 min washes (1 ml each) of ice-cold PBS containing 0.1 or 0.05 M galactose. The remaining cell-associated label, measured as described above, was considered intracellular.

Alternatively, cells that had bound [^{125}I]RCAI at 4°C for 20 min were rinsed well and warmed to 37°C in SFM/BSA to allow internalization to proceed. At selected time intervals, the medium was decanted, the cells rinsed with ice-cold PBS and the surface-associated [^{125}I]RCAI removed with galactose. The stripped cells then were solubilized to measure the fraction of bound [^{125}I]RCAI that had been endocytosed.

Degradation of the [^{125}I]RCAI was assessed by determining the amount of radioactivity that was soluble in 10% (w/v) trichloroacetic acid (TCA). To each sample was added 0.1 mg ml^{-1} BSA as a carrier. Alternatively, degradation was measured by the percentage of radioactivity that passed through a 10^4 M_r cutoff Centricon-10™ filter (Amicon Corp., Danvers, MA).

The effects of exposure to RCAI on cell viability under the conditions described herein were examined. Confluent cultures were either pulse labeled with 0–50 μg ml^{-1} RCAI for 30 min at 4°C, rinsed and incubated for 2 h at 37°C, or incubated continuously with 0–50 μg ml^{-1} RCAI. After rinsing, the viability of cells in these cultures was determined by using fluorescein diacetate and ethidium bromide (Carson and Haudenschild, 1986).

Recycling of accumulated [^{125}I]RCAI

Cells that had been allowed to accumulate [^{125}I]RCAI as described above were chilled and the surface-bound lectin removed with 0.1 M galactose. Washed cells were rewarmed to 37°C in SFM/BSA with or without 0.05 M galactose. Efflux was measured for up to 60 min by determining the amount of TCA-insoluble radioactivity that had returned to the cell surface. The cells were then solubilized to measure the amount of cell-associated radioactivity that was not recycled or released by galactose.

Radiolabel incorporation into cellular proteins

After incubating cell monolayers in SFM for 1 h at 37°C, cell surface components of intact BMECs were labeled with ^{125}I by using lactoperoxidase according to Hubbard and Cohn (1975). Alternatively, BMECs grown in 100-mm dishes were preincubated in minimum essential medium (MEM) without glutamine and glucose (Gibco Laboratories, Grand Island, NY), and after 30 min the medium was replaced with 5 ml of glucose-free MEM containing 50 μCi ml^{-1} D-[1,6-^{3}H(*N*)]glucosamine hydrochloride (42.5 Ci mmol^{-1}; New England Nuclear, Boston, MA). After 3–5 h at 37°C, an additional 5 ml of complete culture medium were added and the incubation continued for 5–14 h. The labeled cells were rinsed well, incubated for an additional hour and then lysed as described below.

Affinity isolation of RCAI binding proteins

Radiolabeled cells were rinsed with ice-cold PBS and incubated for 1 h at 4°C in TBS (0.02 M Tris–HCl, pH 8, 0.15 M NaCl) containing 1% (w/v) deoxycholic acid (DOC), 0.001 M ethylenediaminetetraacetic acid (EDTA), 0.001 M phenylmethylsulfonyl fluoride (PMSF), 1 μg ml^{-1} leupeptin, 0.2 t.i.u. ml^{-1} aprotinin and

0.02% (w/v) sodium azide. After the lysate was clarified by centrifugation at 11 000 *g* for 5 min, TCA-insoluble radioactivity was determined by soaking lysate-spotted glass fibre filters in 10% (w/v) TCA containing 0.05 M glucosamine (Hubbard and Cohn, 1975).

The lysates were passed through a column of 5 ml of agarose-bound RCA_{120} (4 mg ml^{-1}; Vector) equilibrated in TBS containing 0.5% (w/v) DOC. After rinsing with 20 column volumes of TBS, bound material was eluted with 2 column volumes of TBS containing 0.5 M galactose. Both bound and unbound fractions were dialyzed against distilled water containing 1 mM PMSF and sodium azide and lyophilized prior to analysis by gel electrophoresis.

Gel electrophoresis

The RCAI-bound and -unbound fractions of radiolabeled cell lysates were reconstituted and boiled in reducing buffer before subjecting them to one-dimensional SDS–polyacrylamide gel electrophoresis (1D-SDS-PAGE) according to Laemmli (1970). Gels were fixed, Coomassie Blue stained, treated with Enlightning™ (New England Nuclear) ([^{3}H]glucosamine only) and dried prior to exposure to XAR-5 X-ray film (Eastman Kodak Co., Rochester, NY) at −70°C ([^{3}H]*glucosamine*) or at 25°C with a Cronex Quanta III™ (E.I. du Pont Nemours & Co., Wilmington, DE) intensifying screen (^{125}I).

Autoradiograms of the bound proteins were analyzed by using the Visage 110 System (BioImage, Ann Arbor, MI). Each lane was scanned using a Kodak 1024×1024 two-dimensional array camera and image analysis was carried out using Visage System software.

Fluorescence microscopy

Bovine BMECs grown to confluence in plastic 2-chamber Lab Tek™ Chamber/Slides (Miles Scientific, Inc., Naperville, IL) were treated as above and incubated for 30 min at 4°C in PBS with 50 μg ml^{-1} fluorescein isothiocyanate (FITC)–lectin (Vector). Control cells were labeled in the presence of 0.2 M of the haptene sugar (Sigma Cemical Co., St Louis, MO). In experiments where lectin internalization was observed, cells were incubated with 25 μg ml^{-1} FITC–lectin in serum-free medium at 37, 18 and 4°C with or without 0.1 M hapten sugar. Labeled cells were fixed at 4°C for 30 min in 4% (w/v) paraformaldehyde in PBS, mounted in 80% (v/v) glycerol in PBS, and viewed with epifluorescence.

Internalization of RCAI conjugates and HRP

Confluent BMECs monolayers in chamber/slides were chilled on ice, thoroughly rinsed with PBS, and incubated with 25 μg ml^{-1} HRP–RCAI (Sigma) or 5.7 μg ml^{-1} of gold (10 nm)–RCAI (E-Y Laboratories, San Mateo, CA) for 30 min at 4°C. Control cells were incubated either with unlabeled RCAI or with conjugate in the presence of 0.1 M galactose. Cells were washed free of unbound label and either processed immediately for electron microscopy or warmed to 37°C in SFM for selected time intervals prior to processing. For HRP accumulation, cell monolayers were incubated in complete medium containing 1 mg ml^{-1} HRP (type I; Sigma). In the uptake experiments, control cells were maintained at 4°C to prevent internalization.

Electron microscopy

Labeled cell monolayers were washed with ice-cold PBS and fixed for 30 min with 2.5% (v/v) glutaraldehyde (Polysciences, Inc., Warrington, PA) in 0.1 M sodium cacodylate buffer, pH 7.4. Cells labeled with HRP were treated as described previously (Raub *et al.* 1990*a*). Washed cell monolayers were post-fixed for 1 h in 2% (w/v) OsO_4 with or without 1% (w/v) potassium ferricyanide in 0.1 M sodium cacodylate, pH 7.4, dehydrated through a graded series of ethanol, and embedded in dish in Poly/Bed™ 812 (Polysciences) (Luft, 1961). Sections of 60–80 nm thickness were mounted on 0.25% (w/v) Formvar-coated grids, doubly post-stained (Reynolds, 1963), and viewed by using a JEOL 1200EX electron microscope operated at 60 kV.

Binding and distribution of the gold–RCAI conjugate was quantified from micrographs by counting the number of gold particles that were associated with the apical plasma membrane, caveolae, intracytoplasmic vesicles, endosomes and the basolateral membrane. Particle densities were determined by expressing the number of particles per μm of membrane that was measured from micrographs at constant magnification (×100 000) by using Sigma-Scan™ (Jandel Scientific, Corte Madera, CA).

Results

Lectin binding to BMECs in vitro

We began this study by surveying a number of lectins (Table 1) that recognize a wide variety of monosaccharides. Our intention was to identify a lectin that had the largest number of apparent binding sites on the BMEC surface for use as a general adsorptive tracer of plasma membrane (glycoprotein and glycolipid) traffic in these cells. Relative fluorescence intensities (Table 1) were judged by fluorescence microscopy following incubation of confluent BMEC monolayers with FITC–lectin. All of the lectins were used at a similar concentration (0.42–0.45 μM) except for *Ulex europaeus* agglutinin I (UEAI) (0.3 μM) and wheat germ agglutinin (WGA) (1.4 μM). Since there was no correlation between the intensity of staining and the concentration of fluorescein used (calculated from the fluorescein/protein ratio of each lectin), which varied from 1.1 to 3.2 μM fluorescein, we suggest that the relative intensities were due to the density of cell surface binding sites. All of the control cells that were labeled in the presence of 0.2 M of the haptene sugar (Table 1) failed to bind lectin (results not shown). Both RCAI and soy bean agglutinin (SBA) bound with the greatest intensity and indicated that the cultured BMEC surface is rich in D-galactose and D-*N*-acetylgalactosamine residues. In contrast, the absence of either UEAI or *Dolichos biforus* aggutinin (DBA) binding suggested that RCAI and SBA recognized primarily the β configuration.

All of the lectins that bound to BMECs at 4°C displayed a uniformly punctate distribution on the cell surface as viewed by fluorescence microscopy (results not shown). By using HRP–lectin conjugates and electron microscopy, the bound lectins were confined to the luminal or apical plasma membrane, which suggested that the conjugate was excluded by the tight junctions. The lectin conjugates also labeled caveolae (see Fig. 6, below).

Table 1. *Relative fluorescence intensities of FITC–lectins that had bound to confluent (day 10) BMECs*

Agglutinin	Sugar specificity	Relative intensity
Ulex europaeus I (UEAI)	α-L-Fucose	−
Dolichos bifuros (DBA)	α-D-GalNAc, α-D-Gal	−
Concanavalin A (Con A)	α-D-Man, α-D-Glc, α-D-GlcNAc	+
Peanut (*Arachis hypogaea*) (PNA)	β-D-Gal(1-3)-D-GalNAc	+
Wheat germ (WGA)	β-D-GlcNAc, NA	++
Soy bean (*Glycine max*) (SBA)	α-D-GalNAc, β-D-GalNAc, β-D-Gal	+++
Ricinus communis I (RCAI)	β-D-Gal, β-D-GalNAc	+++

Washed cell monolayers were incubated with 50 μg ml^{-1} FITC–lectin for 30 min at 4°C, rinsed, fixed with 4% paraformaldehyde and viewed with epifluorescence microscopy. Relative intensity: (−) none, (+) weak, (++) moderate, (+++) strong.

Abbreviations: Gal, galactose; GalNAc, *N*-acetylgalactosamine; Glc, glucose; GlcNAc, *N*-acetylglucosamine; Man, mannose; NA, neuraminic acid.

Binding and release of RCAI from cultured BMECs

To establish the conditions at which subsequent internalization experiments were to be done, the kinetics of RCAI–BMEC interactions were examined. Both the association rate at 4°C and the dissociation rate at 37°C were determined and both were at steady-state after 20 min (results not shown). For dissociation, paraformaldehyde-fixed cells were used to measure kinetics at 37°C without accompanying endocytosis. Under these conditions, as much as 45 % of the RCAI that had bound at 4°C was lost into the medium within 30 min. Using pseudo-first order kinetics (Owensby *et al.* 1989), the 'off' rate had a $t_{\frac{1}{2}}$ of 4 min. The 'on' rate was determined to have a $t_{\frac{1}{2}}$ of 6 min. For dissociation, a similar value was observed during internalization (see Fig. 4, below), suggesting that fixation did not alter the kinetics. In all cases, three quick rinses with PBS at 4°C were sufficient to remove all of the unbound lectin.

After incubation for 20 min at 4°C, saturation was reached at 15 $\mu g\,ml^{-1}$ (Fig. 1). By using [^{125}I]RCAI (5 nM) either with increasing concentrations of unlabeled RCAI or in the presence of 0.1 M galactose, we found that 94–96 % of the binding was specific. Similar results were obtained using capillary endothelia derived from bovine adrenal (results not shown). The surface-bound RCAI was removed rapidly and quantitatively with 93(±2)% efficiency by using two, 5-min rinses with 0.05–0.1 M galactose at 4°C. RCAI that had associated with BMECs at 37°C gradually became inaccessible for removal by galactose. This provided a way of distinguishing between RCAI at the cell surface and that which had been internalized by the cells.

Identification of RCAI binding proteins on the BMEC surface

Cell surface glycoproteins that bound RCAI were identified by using whole-cell radioiodination followed by lectin-affinity chromatography. Labeled proteins that had bound to immobilized RCAI were eluted with galactose and analyzed by 1D SDS–PAGE and autoradiography. Of the proteins that were iodinated in intact cells, 76 % of the TCA-insoluble radioactivity bound RCAI (Fig. 2). Following incorporation of [^{3}H]glucosamine, 59 % of the TCA-insoluble radioactivity bound RCAI (results not shown). In contrast, only 3.5 % and 4.2 % of the TCA-insoluble [^{35}S]methionine- and [^{3}H]leucine-labeled radioactivity bound RCAI (results not shown). In all cases, the same major RCAI-binding proteins were observed at 180–185, 155, 135–140, and 115–120$\times10^{3}$ M_r (Fig. 2).

The relative amounts of these glycoproteins, especially those greater than 120$\times10^{3}$ M_r, increased with age in culture without an increase in cell number. A significant change in composition was not observed (Fig. 2). We also compared the expression of four of the RCAI binding proteins that had been labeled with [^{3}H]glucosamine between primary BMECs (day 14 of culture), few (pass 4) and many (pass 12) passaged primary BMECs, passaged bovine adrenal endothelia, and bovine kidney epithelia (MDBK). A 185$\times10^{3}$ M_r glycoprotein was lost in the many passaged BMECs and also was absent in MDBK. In contrast, a 165$\times10^{3}$ M_r glycoprotein that was absent in primary BMECs was found in few and many passaged BMECs and in MDBK (results not shown).

Endocytosis of RCAI by BMECs

The kinetics of lectin–membrane internalization were studied by using both a continuous incubation at 37°C with [^{125}I]RCAI (2.5 nM) and a pulse-label at 4°C followed by a 'chase' at 37°C. The distribution of RCAI in continuously incubated cells was determined by using a galactose wash at 4°C to distinguish surface-bound RCAI from that which had been internalized (Fig. 3). Pseudo-first-order kinetics gave a $t_{\frac{1}{2}}$ of 5 min for the rate at which RCAI became cell surface associated. In comparison, the $t_{\frac{1}{2}}$ for RCAI accumulation into a galactose-resistant form was 18 min. Both binding and subsequent intracellular accumulation gradually decreased to a steady-state rate with a $t_{\frac{1}{2}}$ of 78 min. This decrease in the accumulation rate was not due either to depletion of the lectin or to a decrease in endocytic activity, since endocytosis of Lucifer Yellow remained unchanged following incubation with RCAI (results not shown). Furthermore, under these conditions RCAI was not toxic to the BMEC, since viability did not differ from untreated cultures.

During continuous incubation, RCAI binding and endocytosis were inhibited by the presence of 0.05 M galactose in the serum-free medium. After 2 h, only 5–6 % of the RCAI was accumulated, most likely by fluid-phase endocytosis (Fig. 3). Furthermore, internalization was inhibited completely at 4°C and was reduced by 65–75 % in the presence of 50 mM 2-deoxyglucose and 5 mM sodium azide (results not shown).

For pulse–chase experiments, cells were allowed to bind subsaturating concentrations of RCAI (<5 nM) for 20 min at 4°C, rinsed and warmed to 37°C in the absence of lectin to allow endocytosis to proceed (Fig. 4). Pseudo-first-order kinetics gave a $t_{\frac{1}{2}}$ of 14 min for the rate of internalization.

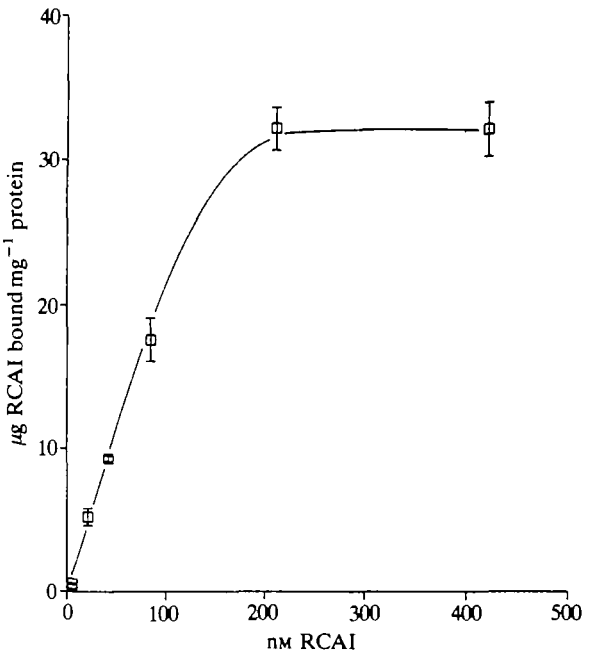

Fig. 1. Saturation curve of RCAI binding to confluent BMECs monolayers at 4°C. Cells at day 10 in culture were incubated with 5 nM [^{125}I]RCAI and increasing amounts of unlabeled RCAI for 20 min at 4°C. After rinsing, the cells were solubilized and the amount of radioactivity that had bound was measured. Total cellular protein per well was determined as described in the text and was corrected for the amount contributed by the extracellular matrix used to coat the growth surface. The means and standard deviations from triplicate wells were corrected for the amount of RCAI that bound in the presence of 0.1 M galactose.

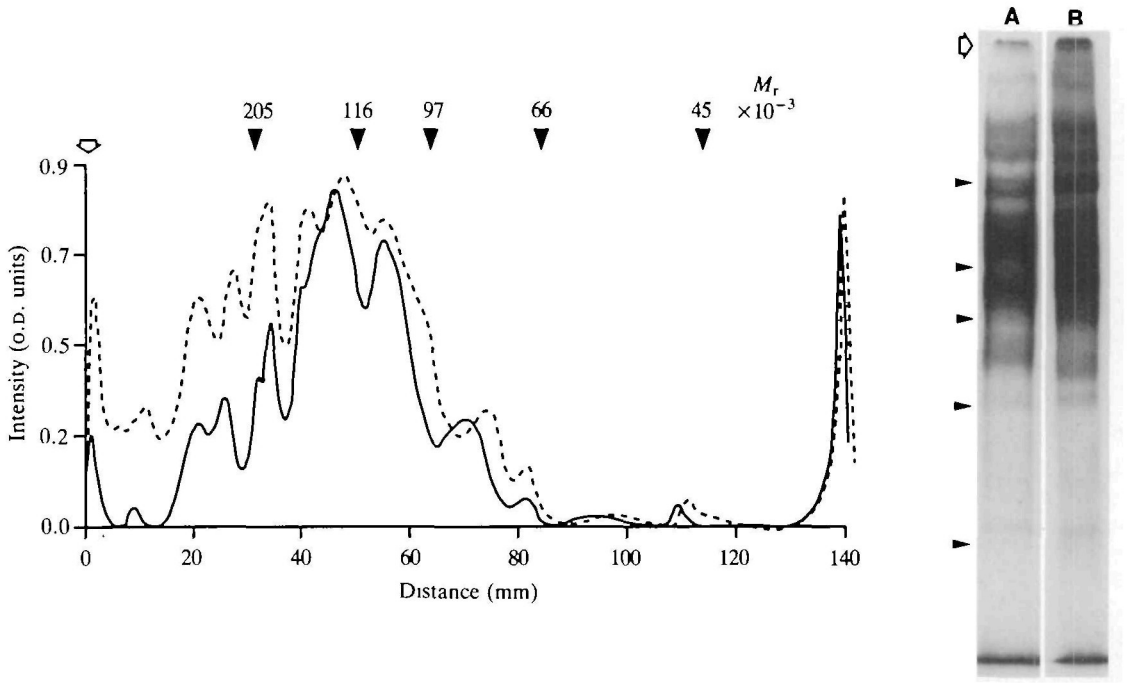

Fig. 2. Densitometric scan of RCAI binding proteins from BMECs that had been radiolabeled by lactoperoxidase-catalyzed iodination. Intact BMECs at day 8 (lane A and continuous line) and day 14 (lane B and broken line) in culture were labeled with ^{125}I, detergent-solubilized and the lysate passed through a column of RCAI–agarose. Bound proteins were eluted with 0.5 M galactose, dialyzed, lyophilized and 50 000 cts min^{-1} (acid-insoluble) subjected to reducing 1D-SDS–PAGE followed by autoradiography. The autoradiograms (lanes A and B) were scanned from top (open arrow) to bottom by image analysis as described in Materials and methods and plotted *versus* molecular weight markers (arrowheads).

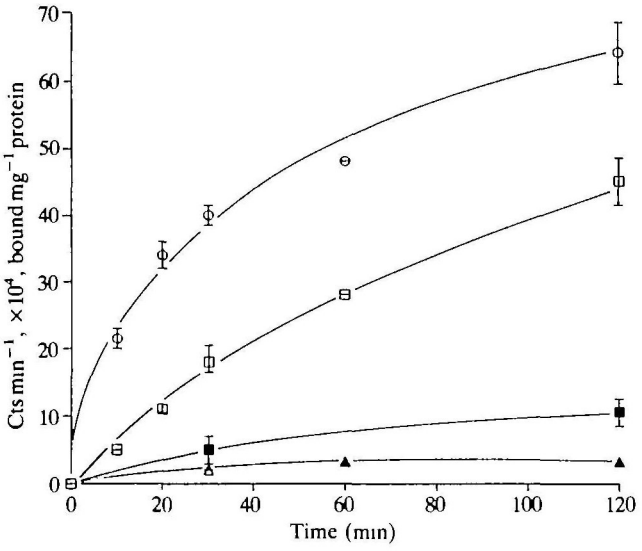

Fig. 3. Time course for binding and accumulation of RCAI by confluent BMEC monolayers during continuous exposure. Cells at day 12 in culture were incubated at 37°C (○,□,△) or 4°C (■) in serum-free medium with 2.5 nM [^{125}I]RCAI. At selected times, cells were rinsed in ice-cold PBS and the amounts of lectin that were intracellular (□,■,△) or at the cell surface (○) were distinguished by using two, 5-min rinses with 0.1 M galactose. Endocytosis of RCAI was inhibited at 4°C (■) and at 37°C in the presence of 0.05 M galactose (△). The values represent the means and standard deviations from 3–6 sets of triplicate wells. All values were normalized to total cellular protein and were corrected for nonspecific binding in the presence of galactose.

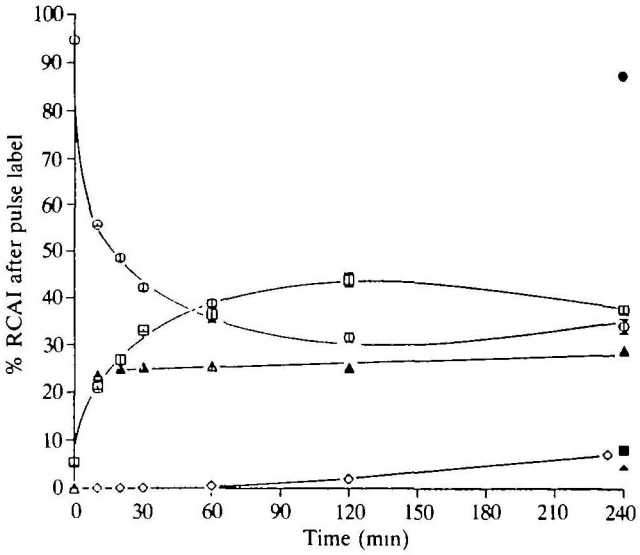

Fig. 4. Fate of RCAI that had bound to confluent BMEC monolayers after warming the labeled cells to 37°C. Cells at day 12 in culture were allowed to bind [^{125}I]RCAI as described for Fig. 1, rinsed well, and warmed to 37°C in serum-free medium. At selected times, the amounts of RCAI that (1) appeared in the medium (△,▲); (2) were at the cell surface (○,●), which was determined by removal with 0.1 M galactose; and (3) were intracellular (□,■), were measured as a fraction of the radioactivity that had been cell-associated. Control cells that were maintained at 4°C (●,■,▲) did not accumulate RCAI. Only a small fraction of the bound RCAI was degraded gradually as shown by the appearance of radioactivity in the medium (◇) that either passed through a $10^4 M_r$ cutoff filter or was soluble in 10% (w/v) TCA.

Within 1 h, 35–40 % of the cell-associated radioactivity was at equilibrium with intracellular compartments. The rapid loss from the cell surface fraction was a sum of that portion internalized and that which dissociated prior to endocytosis.

Degradation of RCAI was measured by the amount of TCA-soluble radioactivity or the amount of radioactivity that passed through a 10×10^3 M_r molecular weight cut-off filter. Degradation was temperature-dependent and was not detected until after 30 min at 37 °C when low molecular weight radioactive fragments gradually began to appear. Less than 7 % of the cell-associated RCAI was degraded during 4 h at 37 °C (Fig. 4).

The endocytic pathway

To correlate our kinetic results using [^{125}I]RCAI with morphology, we used FITC–, HRP– and gold–conjugates of RCAI in parallel experiments and assumed that these conjugates behaved like the native lectin. Internalization was followed by fluorescence and electron microscopy after pulse labeling at 4 °C. We initially established that surface-bound FITC–RCAI became localized within compartments that were refractory to the galactose wash (Fig. 5). At 18 °C, a temperature that inhibits post-endosome events (Sandvig and Olsnes, 1979; Dunn *et al.* 1980), lectin was internalized, but the RCAI-containing vesicles were smaller in size and were more numerous (Fig. 5B) than those at 37 °C (Fig. 5C).

Both HRP– and gold–RCAI were used, since each has advantages in visualizing endocytic compartments. The HRP–conjugate by virtue of its amplified signal is visualized at low concentrations, although resolution of localization is less than for the gold conjugate. Moreover, the HRP–RCAI probe is more like native RCAI, since it is a soluble protein whereas the gold–RCAI probe is an insoluble particle that contains many RCAI molecules per particle. Despite this polyvalency, the gold probe can be used to quantify internalization. By comparing our results qualitatively and quantitatively, both probes behaved alike and similar to unconjugated RCAI.

Ricin agglutinin I conjugates that had bound to BMEC

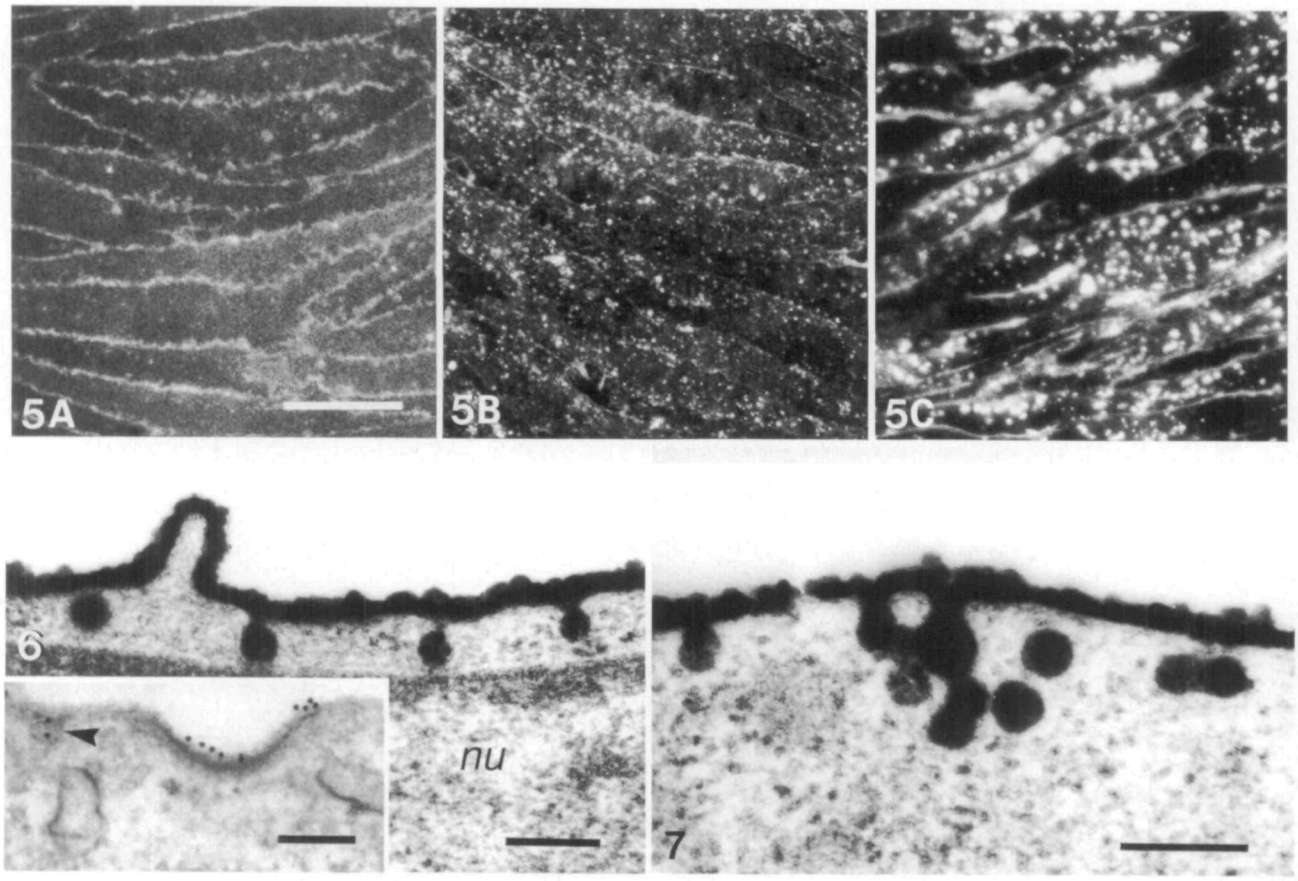

Fig. 5. Binding and internalization of RCAI by confluent BMEC monolayers was examined by fluorescence microscopy. Cells at day 10 in culture were incubated for 30 min at 4 °C with 0.2 μM FITC–RCAI, rinsed and fixed with paraformaldehyde either immediately (A) or after warming the labeled cells to 18 °C (B) and 37 °C (C). Bar, 20 μm.

Fig. 6. Distribution of RCA binding sites on BMECs was shown by using cell surface-bound RCAI conjugates and electron microscopy. Confluent BMEC monolayers at day 10 in culture were incubated for 30 min at 4 °C with 0.2 μM HRP–RCAI or 0.05 μM gold–RCAI (inset) and processed immediately for cTEM as described in the text. RCAI binding sites were distributed evenly over the entire apical plasma membrane including within caveolae (1–2% of the surface; see Fig. 8). nu, nucleus. Bar, 200 nm. Inset: RCA binding sites also were localized within an occasional clathrin-coated pit and in micropinocytic invaginations (arrowhead). Bar, 100 nm.

Fig. 7. Ultrastructural distribution of BMEC surface RCA binding sites following endocytosis. Within 2.5 min after returning cells that had bound HRP-RCAI to 37 °C, numerous invaginations and putative vesicles that contained lectin were formed and often appeared to be racemose. Cells that had bound HRP–RCAI as in Fig. 6 were rinsed, warmed in serum-free medium, and processed for cTEM. Bar, 200 nm.

at 4°C were found within smooth-membraned invaginations or caveolae that were 70–75 nm in diameter (Figs 6, 7, 9, 11). Although a few coated pits were observed to contain RCAI at 4°C (Fig. 6), these regions were not thought to be involved significantly in endocytosis, since so few invaginated coated pits relative to caveolae were found. Using gold–RCAI, we quantified the specific binding of the lectin as a function of density. There were 17±8 gold particles μm^{-1} plasma membrane after 20 min at 4°C. Control cells that had been labeled in the presence of 0.1 M galactose had only 1.7±0.2 gold particles μm^{-1} plasma membrane. Furthermore, labeled cells that were held at 4°C for an additional 60 min had 9±3 gold particles μm^{-1} plasma membrane.

Immediately after warming to 37°C, the number of labeled caveolae and vesicles at the cell surface increased and were closely associated (Fig. 7). Although these clusters appeared to be interconnected, further attempts to show this unequivocally were not pursued. Fig. 8 shows the quantitative change in distribution of gold–RCAI during endocytosis. These results were consistent with the kinetics obtained using [^{125}I]RCAI (see Fig. 4). Gold–RCAI was lost rapidly from the cell surface and appeared first in caveolae and cytoplasmic vesicles. By 5 min, as much as 43% of the label at the plasma membrane was associated with the stomata or the vesicular 'body' of the caveolae (see Figs 6, 11) compared to only 1–2% prior to endocytosis (Fig. 8). Afterwards, the portion of gold particles in caveolae and vesicles declined and was followed by a gradual increase within endosomes (Fig. 8).

As early as 5 min after warming the labeled cells to 37°C, RCAI became localized within tubules (45 nm diameter) and endosomes (200–400 nm diameter) that were irregular in shape and surrounded by vesicles and tubules (Figs 8–9). The RCAI conjugate within the endosomal lumen was distributed unevenly in association with intraluminal membranes (Fig. 9). The density of gold–RCAI particles per μm of endosomal membrane increased as much as sixfold by 15 min, when an apparent steady state was reached. As endocytosis continued, RCAI conjugate appeared within numerous vesicles and tubules (55–90 nm in diameter) located *trans*-most to the Golgi apparatus between 15 and 30 min (Fig. 10). This distribution contrasted with that of HRP alone, which visualized the fluid-phase endocytic pathway. HRP accumulated within small vesicles of 70 nm in diameter as early as 10 min at 37°C and within endosomes by 30 min; however, at no time was HRP detected within the *trans*-Golgi compartments (results not shown).

Less than 0.1% or 1 in 1000 gold particles of the gold–RCAI was found on the basolateral side of the BMEC monolayer after 60 min at 37°C (Fig. 11). Vesicles that contained lectin conjugate were observed infrequently to be continuous with the basolateral surface (Fig. 11B) or with the lateral membrane at regions lacking the microfilament-associated plaque (results not shown). The density of gold–RCAI that remained at the apical surface had decreased 90% (Fig. 8) by 60 min at 37°C and all was located exclusively within caveolae (Fig. 11).

Recycling of RCAI from a non-degradative compartment

Return of internalized RCAI to the cell surface was examined by allowing cells to accumulate [^{125}I]RCAI to equilibrium (e.g. 60 min), removing the cell surface-associated lectin at 4°C with galactose and re-warming the cells to 37°C with and without galactose present in the medium (Fig. 12). In the presence of galactose, RCAI that returned

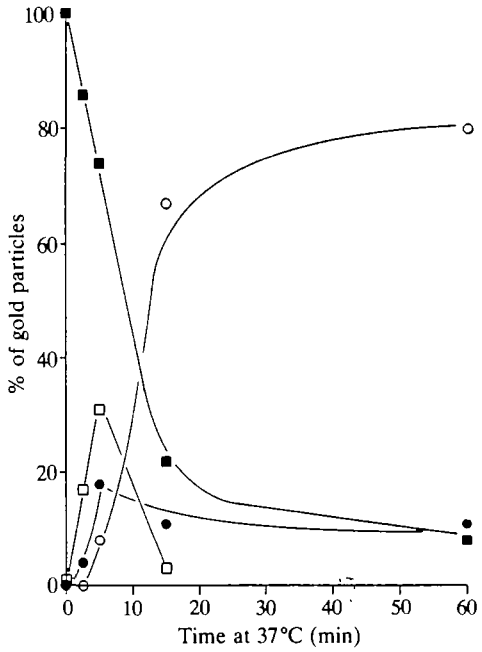

Fig. 8. Kinetics of endocytosis from quantitative morphometry of gold–RCAI distribution. Cells were labeled with gold–RCAI as described for Fig. 6 and either processed immediately (0 min) or warmed to 37°C in serum-free medium for up to 60 min prior to processing for cTEM. More than 300 gold particles were counted for each time point from at least 10 electron micrographs at constant magnification. The location of each gold particle was assigned to plasma membrane (■), caveolae (□), vesicles (●) or endosomes (○), and the results were plotted as a fraction of the total number of gold particles counted.

to the cell surface was removed and, therefore, was unavailable for another round of recycling. In the absence of galactose, this RCAI was re-internalized. By 1 h at 37°C 60% of the intracellular radioactivity was returned gradually to the cell surface in the presence of galactose, 15% in the absence of galactose and 5% in the presence of galactose but at 4°C. In all cases, the radioactivity that appeared within the medium was intact protein. Pseudo-first-order kinetics gave efflux a $t_{\frac{1}{2}}$ of 13.5 min. Using bovine adrenal endothelia, slightly more of the intracellular RCAI was recycled with a twofold increase in rate ($t_{\frac{1}{2}}$=7.5) of efflux (Fig. 12). These results were specific to galactose, since only 24(±2)% and 18(±1)% of the RCAI was returned in the presence of equimolar concentrations of glucose and mannose, respectively (results not shown).

We next asked whether the intracellular pool of recycling RCAI was constant or if a portion was temporally removed to a slowly or non-recycling compartment. We simply varied the length of time allowed for internalization of cell surface-bound [^{125}I]RCAI with the idea that more of the RCAI might enter a latent compartment at the longer times. The rate and extent of efflux was unaffected after accumulation for up to 60 min (results not shown).

Discussion

In recent years, many studies have focused on receptor-mediated endocytosis and transcytosis by endothelia, yet membrane traffic and the extent of recycling remain largely unknown (Davies, 1984; Simionescu, 1988). In this

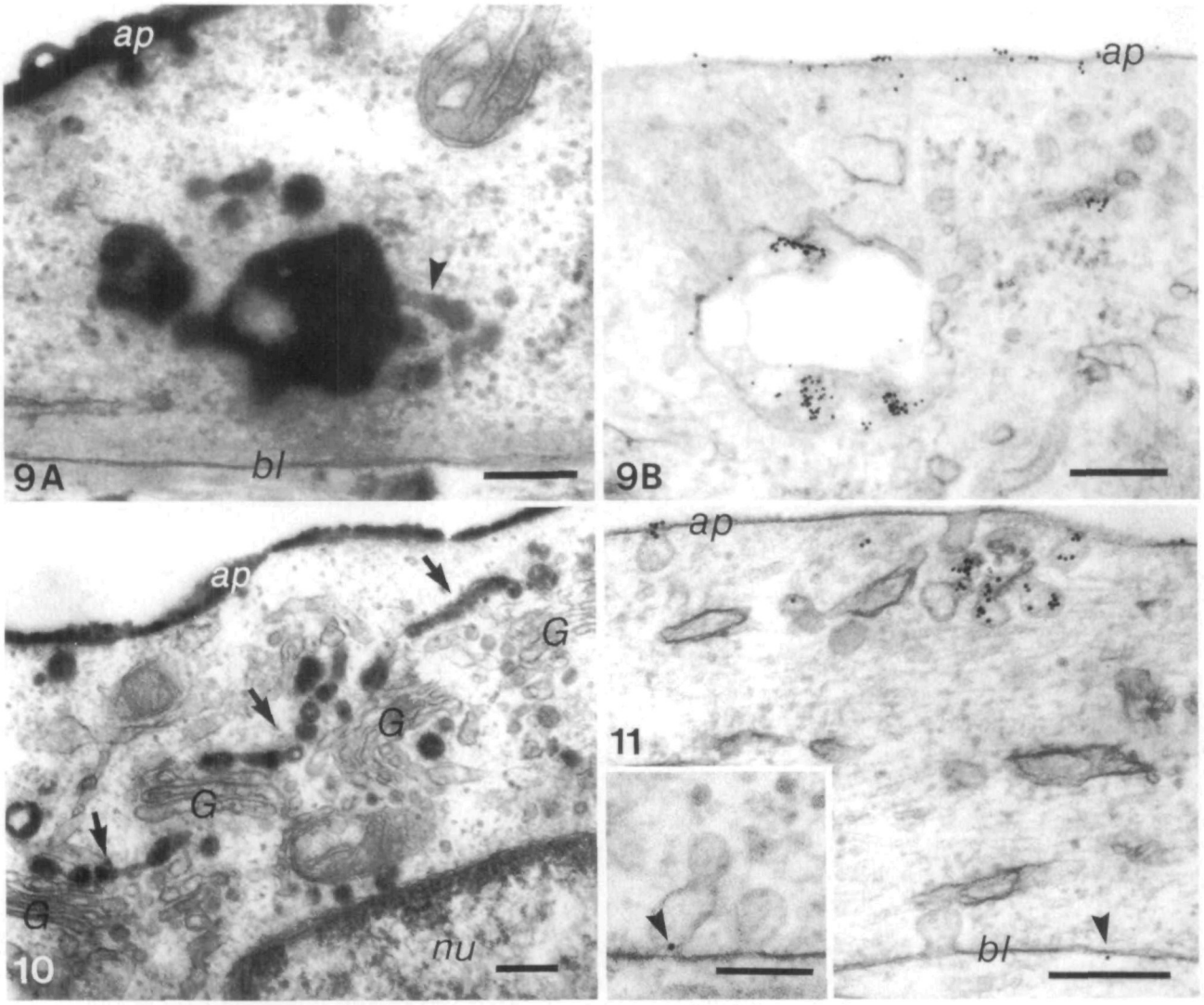

Fig. 9. Ultrastructural distribution of BMEC surface RCA binding sites following endocytosis. Endosomes, vesicles and associated tubules (arrowhead) accumulated RCAI after warming pulse-labeled cells to 37 °C for 15 min. Confluent cell monolayers were treated with either HRP–RCAI (A) or gold–RCAI (B) as described for Fig. 6, rinsed, and warmed in serum-free medium prior to processing for cTEM. Some label remained on the apical membrane (ap) and was absent from the basolateral membrane (bl). Bars, 200 nm.
Fig. 10. Ultrastructural distribution of BMEC surface RCA binding sites following endocytosis. Within 30 min of warming cells to 37 °C as for Fig. 9, a fraction of the apical membrane (ap) bound HRP–RCAI was routed to the *trans*-Golgi network (arrows). Lectin was not localized within the Golgi (G) cisternae *per se*. Bar, 200 nm.
Fig. 11. Ultrastructural distribution of BMEC surface RCA binding sites following endocytosis. After 60 min at 37 °C, most of the apical membrane (ap)-bound gold–RCAI was still associated with caveolae or endosomes (not shown). Only an occasional gold particle (arrowheads) was found on the basolateral membrane (bl) and sometimes was associated with a membrane invagination (inset). This suggested that a very small fraction of the apical membrane RCA binding sites entered a transcytotic route. Inset: bar, 100 nm. Bar, 200 nm.

study, we examined the kinetics of membrane recycling in cultured brain endothelia by measuring the accumulation and efflux of the lectin RCAI. This lectin was chosen because it appeared to have the most binding sites of the lectins tested. We showed that RCAI bound to a subpopulation of cell surface glycoproteins and/or glycoplipids of which the majority cycled between the plasma membrane and several intracellular compartments. At least a portion of these cycling glycoproteins were routed through the *trans*-Golgi network (TGN) (Griffiths and Simons, 1986).

Our results from the survey of lectin binding to cultured BMECs were consistent with the results of others both *in vitro* and *in vivo*. Brain MEC of mouse, rat, canine, bovine, and human stained intensely with RCAI (Nag, 1985; Vorbrodt *et al.* 1986; Gerhardt *et al.* 1986; Fatehi *et al.* 1987; Debbage *et al.* 1988). Also, except for human BMECs (Debbage *et al.* 1988), BMECs of all species were UEAI negative. Also, SBA bound equally as well as RCAI; however, binding apparently is species dependent. While rat BMECs were strongly positive for SBA (Nag, 1985), canine BMECs were weakly positive (Fatehi *et al.* 1987) and human BMECs were negative (Debbage *et al.* 1988). Together, these results suggested that primary cultures of BMECs have a surface composition that is similar to that found *in vivo*.

Expression of the RCAI binding proteins was stable throughout culture with only minor changes. We observed some changes in the RCAI binding proteins of BMECs that

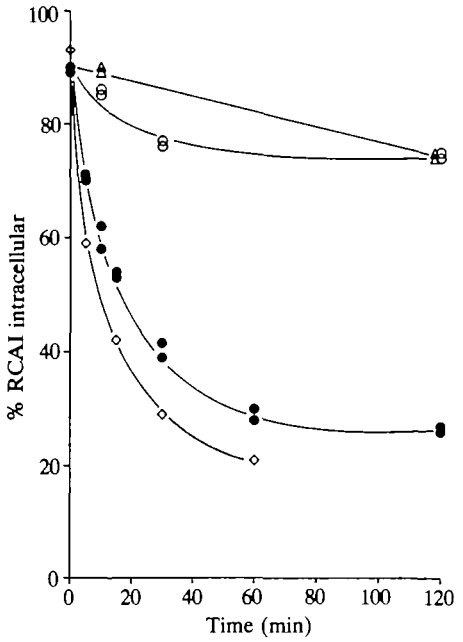

Fig. 12. Efflux of intracellular RCA binding sites from BMEC monolayers (●,○,△) and from bovine adrenal endothelia (◇). Cells that had bound [^{125}I]RCAI at 4°C as for Fig. 3 were allowed to endocytose for 30 min at 37°C. After removal of the remaining surface-bound lectin with ice-cold galactose, the cells were either maintained at 4°C (△) or returned to 37°C in serum-free medium alone (○) or containing 0.05 M galactose (●,◇). At selected times, cells were chilled and treated with galactose, rinsed and solubilized. The intracellular radioactivity was plotted as a fraction of the surface-bound label that was endocytosed. Each data point is the mean of triplicate wells. Standard deviations (not shown) were <5% of the mean.

had been passaged several times in culture. Fatehi *et al.* (1987) also showed that both SBA and DBA binding sites were lost in passaged cells. The avidity of RCAI is not restricted to BMECs, but is a universal feature of most endothelia examined (Simionescu, 1988). Moreover, the caveolar membrane has a high density of galactosyl-rich glycoproteins (Simionescu *et al.* 1982). Since these surface invaginations are most likely involved in endocytosis, this was another reason we chose RCAI as a probe for membrane traffic.

Accumulation and efflux of RCAI were energy-dependent events and were inhibited by low temperature or by metabolic poisons. We showed previously that the majority of fluid accumulation by cultured BMECs was not energy-dependent and that this was consistent with the results of others for endothelia *in vitro* (Guillot *et al.* 1990). Brain MECs have a very low capacity for fluid accumulation and the kinetics of uptake suggest that the majority of cell-associated fluid is within a single compartment of small size that is near to the plasma membrane (Guillot *et al.* 1990). This study could not determine if this compartment was continuous with the plasma membrane or was continually and rapidly detaching and fusing with it. The results in the present study showed that BMECs have a greater capacity to accumulate membrane-adsorbed molecules than solutes. The kinetics of accumulation and efflux for both fluid and membrane recycling were very different, with the latter being much slower. Together, these results suggested that the bulk flow of membrane is designed to minimize contact with blood components, i.e. a short-circuit pathway for fluids, and maximize interaction with specific blood components for subsequent routing through the membrane pathway for self-utilization or for transcytosis. Such a scenario is paramount to barrier function.

These results most likely were not the result of lectin toxicity, e.g. inhibition of protein synthesis, since cell viability was not affected at the lectin concentrations and for the duration of the incubations used here. Moreover, pure RCAI has almost no toxicity like that attributed to ricin toxin (Olsnes *et al.* 1974). We have not ruled out unequivocally, however, that RCAI binding and subsequent internalization were influenced by the lectin itself. For instance, concanavalin A was shown to induce internalization in macrophages (Edelson and Cohn, 1974), but at concentrations greater than 30 $\mu g\,ml^{-1}$. We know that high concentrations of RCAI (10 $\mu g\,ml^{-1}$) increased the amount of Lucifer Yellow that was accumulated by BMECs by 58% after 10 min (F. Guillot, unpublished results). However, at the concentrations (<0.5 $\mu g\,ml^{-1}$) used in these kinetic studies, this effect was minimal. Gonatas *et al.* (1980) found that concentrations of RCAII (RCA_{60}) up to 50 $\mu g\,ml^{-1}$ did not stimulate or inhibit endocytosis in a neuroblastoma cell line. As a general phenomenon in endothelia, others reported that high concentrations (>5 $mg\,ml^{-1}$) of proteins, which presumably are internalized by an adsorptive process, stimulated fluid-phase endocytosis (Williams *et al.* 1981, 1984). Although the concentration of albumin used in this study to prevent nonspecific adsorption of RCAI was much less (1 $mg\,ml^{-1}$), its influence on endocytosis is unknown. Moreover, an influence of albumin on endocytosis by BMECs was less likely, since these endothelia do not possess albumin receptors (Simionescu *et al.* 1988; Smith and Borchardt, 1989).

Because RCAI is bivalent (Olsnes *et al.* 1974), endocytosis may have been induced by cross-linking of cell surface glycoconjugates. Such interactions might have resulted in the routing of the lectin–membrane complexes to compartments not accessed by the recycling membrane alone or in the exclusion of such complexes from the constitutive pathway. For example, cross-linking of the Fc receptor on macrophage resulted in degradation of the ligand–receptor complex within lysosomes (Mellman and Plutner, 1984). Our data showed that only a small quantity of internalized RCA was degraded after prolonged incubation, suggesting that RCA–membrane complexes bypassed the lysosome. This was not surprising, since we showed previously that cultured BMECs have few lysosomes as defined by the localization of acid phosphatase (Baranczyk-Kuzma *et al.* 1989). Another explanation is that RCAI was delivered to lysosomes and either was recycled rapidly through this compartment or was resistant to degradation (Olsnes, 1978; Sandvig and Olsnes, 1978). Our morphological results were consistent with the absence of lysosomal involvement, since HRP–RCAI did not label large, spherical compartments. In contrast, free HRP accumulated within compartments with diameters greater than 500 nm. We expected HRP to be routed to lysosomes if it was truly a nonabsorbed marker in these cells (Steinman and Cohn, 1972). Free HRP does not gain access to the TGN compartment (Gonatas *et al.* 1984; van Deurs *et al.* 1987; Raub *et al.* 1990*a*). Cell fractionation studies are needed to define the involvement of lysosomes in the endocytic pathway of BMECs.

By using the rate constants calculated from the pseudo-first-order rates of binding, internalization and efflux, we

estimated a mean transit time ($t_c=(k_1)^{-1}+(k_2)^{-1}+(k_x)^{-1}$; Owensby *et al.* 1989) of 48 min for cycling of the RCAI-binding sites. At least 80 % of the binding sites were involved. This value may actually be an underestimate, since we could not determine if the remaining 20 % was actually sequestered or just not stripped efficiently by the method employed. Kinetically, there was no evidence for the temporal movement of a fraction of this cycling pool into a second compartment. We also observed this using a fluid-phase marker (Guillot *et al.* 1990). These results were not consistent with results in non-endothelial cells showing that a second compartment exists from which membrane-bound ligands are slowly recycled (Mellman *et al.* 1984; Raub *et al.* 1986; Raub *et al.* 1990*b*). Therefore, most if not all of the cycling RCAI binding sites in BMECs appeared to be routed through one kinetically defined compartment.

Our comparison to passaged bovine adrenal endothelial cells suggested that RCAI efflux was faster and more extensive than in BMECs; however, how that relates to the specialized function of BMECs is uncertain. Similar studies with unpolarized Chinese hamster ovary cells using WGA gave a mean transit time of 35 min (Raub *et al.* 1990*b*). Studies of this kind have not been done with other endothelia, so direct comparisons are impossible. However, kinetic studies using specific ligand–receptor complexes have been done. For example, efflux of insulin from rat epididymal fat endothelial cells had a $t_{\frac{1}{2}}$ of 18 min (Bottaro *et al.* 1989) and is similar to that reported here for efflux of RCAI. Efflux of insulin from isolated brain capillaries had a $t_{\frac{1}{2}}$ of 70 min (Pardridge *et al.* 1985) although most was not energy-dependent and may reflect diffusion from an extracellular space. Efflux of transferrin, which recycles through the TGN (Stoorvogel *et al.* 1988), from isolated rat epididymal fat capillaries was very rapid with 80 % lost within 20 min (Wagner *et al.* 1983). We also measured transferrin efflux from BMECs in primary culture and found a $t_{\frac{1}{2}}$ of 38 min (Raub and Newton, 1990), which is much longer than that in epididymal fat capillaries and shown here for RCAI binding sites. The significance of these differences is unclear, since the effects of isolation procedures and culture conditions on these events are unknown.

We assumed in this study that the RCAI conjugates behaved like native and iodinated RCAI; however, this may not be true for the gold–RCAI. Because it is a polyvalent probe, i.e. many molecules of RCAI per gold particle, subsequent intracellular routing may be altered as discussed above. For instance, while native (^{125}I-labeled) and gold–ricin toxin behaved with similar kinetics during endocytosis (van Deurs *et al.* 1985) the gold–ricin toxin was excluded from the TGN (van Deurs *et al.* 1986). In contrast, the HRP–ricin toxin conjugate was not excluded due presumably to its monovalence (Gonatas *et al.* 1984; van Deurs *et al.* 1986). Our morphological results suggested a similar discrepancy between gold–RCAI and HRP–RCAI. Very little of the gold–RCAI compared to HRP–RCAI was localized within the TGN of BMECs. On the other hand, our morphometric quantitation of gold–RCAI distribution during uptake gave kinetics that were reminiscent of data obtained using [^{125}I]RCAI. This suggested that inaccessibility of gold–RCAI to the TGN had little effect on the kinetics of cycling of most of the RCA-binding site population. This could be interpreted as indicating that the fraction of RCAI binding sites that was routed to the TGN was small. We did not, however, measure efflux of the gold–RCAI conjugate.

Our data showed that a fraction of the RCAI binding sites was routed through the TGN of BMECs. Broadwell *et al.* (1988) also reported the involvement of Golgi-associated compartments in BMECs *in vivo* following endocytosis of HRP–wheat germ agglutinin (WGA) from the apical or blood-side surface. The appearance of HRP–WGA within this compartment took considerably longer (>3 h) than reported here (>30 min) for HRP–RCAI and may reflect differences between cultured cells and those *in situ* or between the respective populations of binding sites. Transcytosis of HRP–WGA to the basolateral surface of BMECs *in vivo* was observed after 6 h (Broadwell *et al.* 1988). We found that only a very small fraction of RCAI conjugates crossed the BMEC monolayer after 2 h although more might be transcytosed with longer incubations.

Although the physiological significance of the transcytotic pathway as seen with lectins is unknown, our results indicated that BMECs in primary culture are polarized. Along with the presence of tight junctions that physically define the apical and basolateral membrane domains (Dragsten *et al.* 1981), BMECs are capable of maintaining functional polarity, despite the fact that RCAI binding sites are present equally on both membrane domains (Vorbrodt *et al.* 1986). We also provided evidence that BMECs maintain a polarized fluid recycling pathway in primary culture (Raub and Newton, 1990). *In vivo*, the apical surface of BMECs is almost exclusively involved in endocytosis as shown following intraventricular administration of HRP (Broadwell *et al.* 1983). Brandli and Simons (1989) recently demonstrated polarized recycling of a subset of galactosylated apical membrane glycoproteins through the TGN of Madin Darby canine kidney epithelial cells. Together, these studies suggest that a mechanism exists for selective endocytosis and sorting to the TGN.

The movement of plasma membrane proteins through the TGN is well documented in many cell types and it is known that this pathway involves only a subset of the total recycling population (Reichner *et al.* 1988; Stoorvogel *et al.* 1988; van Deurs *et al.* 1988; Brandli and Simons, 1989). van Deurs *et al.* (1988) using quantitative immunocytochemistry estimated that 5 % of internalized ricin toxin is in the Golgi region and of that 70–80 % is in the TGN. It was proposed that one route for transcytosis in BMECs might involve the TGN (Broadwell *et al.* 1988). Sorting of apical proteins to the TGN and subsequent entrance into a basolaterally directed, exocytotic pathway could be the mechanism. Such a pathway, albeit a minor one, may explain how cationized proteins, which are nonspecifically adsorbed to the cell surface, are transcytosed in BMECs (Kumagai *et al.* 1987; Triguero *et al.* 1989; Smith and Borchardt, 1989). Indeed, Stoorvogel *et al.* (1988) showed in hepatoma cells that the endocytic and secretory pathways are connected in the TGN.

In conclusion, we have measured the endocytosis and recycling of RCAI binding sites within primary cultures of BMEC monolayers. The majority of internalized binding sites were recycled, relatively slowly compared to a fluid-phase marker (Guillot *et al.* 1990), from what appeared to be a single kinetic compartment. In other words, the data suggested that a second, nonrecycling or more slowly recycling compartment was not involved. Morphologically, the endocytic pathway encountered by these internalized RCAI binding sites involved caveolae, peripheral endosomes and smooth-membraned tubules, and vesicles of which a portion was located in the TGN. Moreover, these internalized RCAI binding sites were not routed to the

basolateral membrane domain under the conditions employed, suggesting that the endocytic membrane pathway is polarized *in vitro* as has been shown *in vivo* (Broadwell *et al.* 1988).

We thank Dr Gospodarowicz for supplying us with the passaged cultures of bovine brain and adrenal microvessel endothelia. We also thank Dr Roger Ulrich for use of the Electron Microscopy facility at The Upjohn Company, Mr Ken Kilgore for technical assistance in the microscopy, and Ms Brenda Mussulman for preparing the manuscript.

References

AUDUS, K. L. AND BORCHARDT, R. T. (1986) Characterization of an *in vitro* blood–brain barrier model system for studying drug transport and metabolism. *Pharm. Res.* **3**, 81–87.

AUDUS, K. L. AND BORCHARDT, R. T. (1987). Bovine brain microvessel endothelial cell monolayers as a model system for blood–brain barrier. *Ann. N. Y. Acad. Sci.* **507**, 9–18

BARANCZYK-KUZMA, A., AUDUS, K. L. AND BORCHARDT, R. T. (1986). Catecholamine-metabolizing enzymes of bovine brain microvessel endothelial cell monolayers. *J. Neurochem.* **46**, 1956–1960

BARANCZYK-KUZMA, A., RAUB, T. J. AND AUDUS, K. L. (1989). Demonstration of acid hydrolase activity in primary cultures of bovine brain microvessel endothelium. *J. cereb. Bl. Fl. and Metab.* **9**, 1–10.

BOTTARO, D. P., BONNER-WEIR, S. AND KING, G. L. (1989). Insulin receptor recycling in vascular endothelial cells. *J. biol Chem.* **264**, 5916–5923.

BOWMAN, P. D., ENNIS, S. R., RAREY, K. E., BETZ, A. L. AND GOLDSTEIN, G. W. (1983). Brain microvessel endothelial cells in tissue culture: a model for study of blood–brain barrier permeability. *Ann. Neurol.* **14**, 396–402.

BRANDLI, A. W. AND SIMONS, K. (1989). A restricted set of apical proteins recycle through the trans-Golgi network in MDCK cells. *EMBO J.* **8**, 3207–3213.

BRIGHTMAN, M. W. (1989). The anatomic basis of the blood–brain barrier. In *Implications of the Blood–Brain Barrier and its Manipulation*, vol. 1 (ed. E. A. Neuwelt), pp. 53–83. New York, London: Plenum Press.

BROADWELL, R. D., BALIN, B. J. AND SALCMAN, M. (1988). Transcytotic pathway for blood-borne protein through the blood–brain barrier. *Proc. natn. Acad. Sci. U.S.A.* **85**, 632–636.

BROADWELL, R. D., BALIN, B. J., SALCMAN, M. AND KAPLAN, R. S. (1983). Brain–blood barrier? Yes and no. *Proc. natn Acad. Sci. U S.A.* **80**, 7352–7356.

CARSON, M. P. AND HAUDENSCHILD, C. C. (1986). Microvascular endothelium and pericytes: high yield, low passage cultures. *In Vitro* **22**, 344–354.

DAVIES, P F. (1984). Quantitative aspects of endocytosis in cultured endothelial cells. In *Biology of Endothelial Cells* (ed. E. A. Jaffe), pp. 365–376. Boston, The Hague: Martinus Nijhoff Publishers.

DEBBAGE, P. L., GABIUS, H.-J., BISE, K. AND MARGUTH, F. (1988). Cellular glycoconjugates and their potential endogenous receptors in the cerebral microvasculature of man: a glycohistochemical study. *Eur. J. Cell Biol.* **46**, 425–434.

DRAGSTEN, P. R., BLUMETHAL, R. AND HANDLER, J. S. (1981). Membrane symmetry in epithelia: is the tight junction a barrier to diffusion in the plasma membrane. *Nature* **294**, 718–722.

DUNN, W. A., HUBBARB, A. L. AND ARONSON, N. N. JR (1980). Low temperature selectively inhibits fusion between pinocytic vesicles and lysosomes during heterophagy of ^{125}I-asialofetuin by the perfused rat liver. *J. biol Chem.* **255**, 5971–5978.

EDELSON, P. J. AND COHN, Z. A. (1974). Effects of concanavalin A on mouse peritoneal macrophages. I. stimulation of endocytic activity and inhibition of phago–lysosome formation. *J. exp. Med.* **140**, 1364–1386.

FATEHI, M. I., GERHARDT, D. Z., MYERS, T. G. AND DREWES, L. R. (1987). Characterization of the blood-brain barrier: glycoconjugate receptors of 14 lectins in canine brain, cultured endothelial cells, and blotted membrane proteins. *Brain Res.* **415**, 30–39.

GERHARDT, D. Z , ZLONIS, M. S. AND DREWES, L. R. (1986). Light and electron microscopic localization of D-galactosyl residues in capillary endothelial cells of the canine cerebral cortex. *J Histochem. Cytochem.* **34**, 641–648.

GOLDSTEIN, G. W., BETZ, A. L. AND BOWMAN, P. D. (1984) Use of isolated brain capillaries and cultured endothelial cells to study the blood–brain barrier. *Fedn Proc. Fedn Am. Socs exp. Biol.* **43**, 191–195.

GONATAS, J., STIEBER, A., OLSNES, S. AND GONATAS, N. K. (1980). Pathways involved in fluid phase and adsorptive endocytosis in neuroblastoma. *J. Cell Biol.* **87**, 579–588

GONATAS, N. K., STIEBER, A., HICKEY, W. F., HERBERT, S. H. AND GONATAS, J. O. (1984) Endosomes and golgi vesicles an adsorptive and fluid phase endocytosis. *J. Cell Biol.* **99**, 1379–1390.

GOSPODAROWICZ, D., MASSOGLIA, S. AND CHENG, J. (1986). Effect of fibroblast growth factor and lipoproteins on the proliferation of endothelial cells derived from bovine adrenal cortex, brain cortex, and corpus luteum capillaries. *J. cell. Physiol.* **127**, 475–484.

GRIFFITHS, G. AND SIMONS, K. (1986). The trans Golgi network: sorting at the exit site of the Golgi complex. *Science* **234**, 438–443.

GUILLOT, F. L., AUDUS, K. L. AND RAUB, T. J. (1990). Fluid-phase endocytosis by primary cultures of bovine brain microvessel endothelial cell monolayers. *Microvasc. Res.* **39**, 1–14.

HUBBARD, A. L. AND COHN, Z. A. (1975). Externally disposed plasma membrane proteins. I. Enzymatic iodination of mouse L cells. *J. Cell Biol.* **64**, 438–460.

KUMAGAI, A. K., EISENBERG, J. B. AND PARDRIDGE, W. M. (1987). Absorptive-mediated endocytosis of cationized albumin and a B-endorphin-cationized albumin chimeric peptide by isolated brain capillaries. *J. biol. Chem.* **262**, 16 214–15 219.

LAEMMLI, U. K. (1970) Cleavage of structural proteins during the assembly of the head of bacteriophage T4. *Nature* **227**, 680–685.

LUFT, J M. (1961). Improvements in epoxy resin embedding methods. *J. biophys. biochem. Cytol.* **9**, 409.

MARKWELL, M. A. K., HAAS, S. M., TOLBERT, N. E. AND BIEBER, L. L. (1981). Protein determination in membrane and lipoprotein samples: manual and automated procedures. *Meth. Enzym.* **72**, 296–303.

MELLMAN, I. AND PLUTNER, H. (1984). Internalization and degradation of macrophage Fc receptors bound to polyvalent immune complexes. *J. Cell Biol.* **98**, 1170–1177.

MELLMAN, I , PLUTNER, H. AND UKKONEN, P (1984). Internalization and rapid recycling of macrophage Fc receptors tagged with monovalent antireceptor antibody: possible role of a prelysosomal compartment. *J. Cell Biol.* **98**, 1163–1169.

NAG, S. (1985). Ultrastructural localization of monosaccharide residues on cerebral endothelium. *Lab. Invest.* **52**, 553–558.

OLSNES, S. (1978). Ricin and ricinus agglutinin, toxic lectins from castor bean. *Meth. Enzym.* **50**, 330–335.

OLSNES, S., SALTVEDT, E. AND PIHL, A. (1974). Isolation and comparison of galactose-binding lectins from Abrus precatorius and Ricinus communis *J biol. Chem.* **249**, 803–810.

OWENSBY, D. A., MORTON, P. A. AND SCHWARTZ, A. L. (1989). Quantitative evaluation of receptor-mediated endocytosis. In *Methods in Cell Biology*, vol. 32 (ed. A. M. Tartakoff), pp 305–328. New York: Academic Press.

PARDRIDGE, W. M. (1988). Recent advances in blood–brain barrier transport. *A. Rev. Pharmac. Toxicol* **28**, 25–39.

PARDRIDGE, W. M., EISENBERG, J. AND YANG, J. (1985). Human blood–brain barrier insulin receptor. *J. Neurochem.* **44**, 1771–1778.

RAUB, T. J., DENNY, J. B. AND ROBERTS, R. M. (1986). Cell surface glycoproteins of CHO cells. I. Internalization and rapid recycling. *Expl Cell Res.* **165**, 73–91.

RAUB, T. J., KOROLY, M. J. AND ROBERTS, R. M. (1990*a*). Endocytosis of wheat germ agglutinin binding sites from the cell surface into a tubular endosomal network. *J. cell. Physiol.* **143**, 1–12.

RAUB, T. J., KOROLY, M. J. AND ROBERTS, R. M. (1990*b*). Endocytosis and recycling of wheat germ agglutinin binding sites on CHO cells: Evidence for two compartments in a nondegradative pathway. *J. cell Physiol.* (in press)

RAUB, T. J. AND NEWTON, C. R. (1990). Membrane recycling, adsorptive and receptor-mediated endocytosis by primary bovine cerebral microvessel endothelial cell monolayers *in vitro*. In *Pharmaceutical Applications of Cell and Tissue Cultures* (ed. G. Wilson, S. S. Davis, and L. Illum) (in press). New York, London: Plenum Press.

REESE, T. S. AND KARNOVSKY, M. J. (1967), Fine structural localization of a blood-brain barrier to exogenous peroxidase. *J. Cell Biol.* **34**, 207–217

REICHNER, J. S., WHITEHEART, S. W. AND HART, G. W. (1988). Intracellular trafficking of cell surface sialoglycoconjugates. *J. biol. Chem.* **263**, 16 316–16 326.

REYNOLDS, E. S. (1963). The use of lead citrate at high pH as an electron opaque stain in electron microscopy. *J. Cell Biol.* **17**, 208–212.

SANDVIG, K. AND OLSNES, S. (1979). Effect of temperature on the uptake, excretion and degradation of abrin and ricin by HeLa cells. *Expl Cell Res.* **121**, 15–25.

SIMIONESCU, M. (1988). Receptor-mediated transcytosis of plasma molecules by vascular endothelium. In *Endothelial Cell Biology in Health and Disease* (ed. N. Simionescu and M. Simionescu), pp. 69–104. New York, London: Plenum Press.

SIMIONESCU, M., GHINEA, N., FIXMAN, A., LASSER, M., KUKES, L., SIMIONESCU, N. AND PALADE, G. E. (1988). The cerebral microvasculature of the rat: structure and luminal surface properties during early development. *J. submicrosc. Cytol. Path.* **20**, 243–261.

SIMIONESCU, M., SIMIONESCU, N. AND PALADE, G. E. (1982).

Differentiated microdomains on the luminal surface of capillary endothelium: distribution of lectin receptors. *J. Cell Biol.* **94**, 406–413.
SMITH, K. R. AND BORCHARDT, R. T. (1989). Permeability and mechanism of albumin, cationized albumin, and glycosylated albumin transcellular transport across monolayers of cultured bovine brain capillary endothelial cells. *Pharm. Res.* **6**, 466–473.
STEINMAN, R. M. AND COHN, Z. A. (1972). The interaction of soluble horseradish peroxidase with mouse peritoneal macrophages *in vitro*. *J. Cell Biol.* **55**, 186–204.
STOORVOGEL, W., GEUZE, H. J., GRIFFITH, J. M. AND STROUS, G. J. (1988). The pathways of endocytosed transferrin and secretory protein are connected in the trans-Golgi reticulum. *J. Cell Biol.* **106**, 1821–1829.
TRIGUERO, D., BUCIAK, J. B., YANG, J. AND PARDRIDGE, W. M. (1989). Blood–brain barrier transport of cationized immunoglobulin G: Enhanced delivery compared to native protein. *Proc. natn. Acad. Sci. U.S.A.* **86**, 4761–4765.
VAN DEURS, B., PEDERSON, L. R., SUNDAN, A., OLSNES, S. AND SANDVIG, K. (1985). Receptor-mediated endocytosis of a ricin-colloidal gold conjugate in vero cells. *Expl Cell Res.* **159**, 287–304.
VAN DEURS, B., PETERSON, O. W., OLSNES, S. AND SANDVIG, K. (1987). Delivery of internalized ricin from endosomes to cisternal Golgi elements is a discontinuous, temperature-sensitive process. *Expl Cell Res.* **171**, 137–152.
VAN DEURS, B., SANDVIG, K., PETERSEN, O. W., OLSNES, S., SIMONS, K. AND GRIFFITHS, G. (1988). Estimation of the amount of internalized ricin that reaches the trans-Golgi network. *J. Cell Biol* **106**, 253–267.
VAN DEURS, B., TONNESSEN, T. I., PETERSON, O. W., SANDVIG, K AND OLSNES, S. (1986). Routing of internalized ricin and ricin conjugates to the Golgi complex. *J. Cell Biol.* **102**, 37–47.
VORBRODT, A. W., DOBROGOWSKA, D. H., LOSSINSKY, A. S. AND WISNIEWSKI, H. M. (1986). Ultrastructural localization of lectin receptors on the luminal and abluminal aspects of brain micro-blood vessels. *J. Histochem. Cytochem.* **34**, 251–261.
WAGNER, R. C., ROBINSON, C. S., CROSS, P. J. AND DEVENNY, J. J. (1983). Endocytosis and exocytosis of transferrin by isolated capillary endothelium *Microvasc Res.* **25**, 387–396
WILLIAMS, S. K., DEVENNY, J. J. AND BITENSKY, M. W (1981) Micropinocytic ingestion of glycosylated albumin by isolated microvessels: possible role in pathogenesis of diabetic microangiopathy. *Proc. natn. Acad. Sci. U.S A.* **78**, 2393–2397.
WILLIAMS, S. K., GREENER, D. A. AND SOLENSKI, N. J. (1984). Endocytosis and exocytosis of protein in capillary endothelium. *J. cell. Physiol.* **120**, 157–162.

(Received 9 March 1990 – Accepted 17 April 1990)